Author Contributions:
Conceptualization: Vivien Wendt
Data curation: Mark A. Clilverd, Tero Raita
Formal analysis: Vivien Wendt
Investigation: Helen Schneider, Daniela Banyś
Methodology: Vivien Wendt, Helen Schneider, Marc Hansen, Mark A. Clilverd
Project administration: Daniela Banyś
Resources: Mark A. Clilverd, Tero Raita
Software: Vivien Wendt, Helen Schneider, Daniela Banyś
Validation: Daniela Banyś
Visualization: Vivien Wendt
Writing – original draft: Vivien Wendt
Writing – review & editing: Vivien Wendt, Helen Schneider, Daniela Banyś, Marc Hansen, Mark A. Clilverd, Tero Raita

Why Does the October Effect Not Occur at Night?

Vivien Wendt[1] , Helen Schneider[1] , Daniela Banyś[1], Marc Hansen[1], Mark A. Clilverd[2] , and Tero Raita[3]

[1]German Aerospace Center, Institute of Solar-Terrestrial Physics, Neustrelitz, Germany, [2]British Antarctic Survey (UKRI-NERC), Cambridge, UK, [3]Sodankylä Geophysical Observatory, University of Oulu, Sodankylä, Finland

Abstract The October effect is known as a rapid and strong decrease in the signal amplitude of radio waves with very low frequency (VLF), reflected at the lowest edge of the ionosphere. This strong decrease can be observed only during the daytime. Although the October effect is long known, it is hardly investigated and its mechanism is still unknown. To get closer to a mechanism, we answer why the October effect does not occur during nighttime. Therefore, average characteristics of the October effect are obtained from different VLF transmitter-receiver combinations. The occurrence of the October effect is then compared with characteristics of the neutral atmosphere temperature at VLF reflection heights as it seems to act as a proxy for the unknown mechanism. The temperature shows an asymmetric seasonal behavior at daytime VLF reflection heights poleward of 50°N but not during the nighttime, resulting in the October effect.

Plain Language Summary The October effect is known as a rapid and strong decrease in the signal amplitude of radio waves with very low frequency, reflected at the lowest edge of the ionosphere (60–90 km). This strong decrease can be observed only during the daytime. Although the October effect has been long known, it is hardly investigated and its mechanism is still unknown. To get one step closer to a mechanism, we want to answer the question of why the October effect does not occur during nighttime. There are two main reasons why the October effect does not occur during nighttime. First, the radio wave reflection height is at around 70 km during daytime and at 85 km during nighttime. The second is the different behavior of the temperature at these two altitudes. While the temperature follows the seasonal cycle of the sun at 85 km, it shows an asymmetric behavior between spring and autumn at 70 km. This unexpected behavior of the temperature at 70 km leads to the October effect during the daytime only.

1. Introduction

Subionospheric radio waves with Very Low Frequency (VLF; 3–30 kHz) are reflected at the lowest edge of the ionosphere which can be typically found at heights around 70 km during daytime and around 85 km during nighttime (Chapman & Macario, 1956). This region of the Earth's atmosphere is called the D-region (50–90 km) and forms the ceiling of the Earth-ionosphere waveguide for VLF radio waves (Wait & Spies, 1964). Due to the low attenuation within the VLF frequency range, the VLF radio signal can propagate thousands of kilometers within the Earth-ionosphere waveguide (e.g., Barr, 1971). The reflected VLF signal's phase and amplitude depend on the D-region's ionization level. While the D-region is mainly ionized by photo-ionization of nitric oxide by Lyman-α radiation and galactic cosmic rays (e.g., Banks & Kockarts, 1973) this process can be disturbed by space weather phenomena like solar flares (e.g., Clilverd et al., 2010) as well as by dynamical and chemical effects from the neutral atmosphere (e.g., Thomson & Clilverd, 2000).

The October effect is well known as a rapid and strong decrease in the daytime VLF signal amplitude in October (e.g., Pancheva & Mukhtarov, 1996). Although the effect has been known for several decades, neither its characteristics (start day, length, magnitude, occurrence region, …) nor its mechanism is known. To the author's knowledge, the only study investigating the October effect more closely is Macotela et al. (2021). Note that Macotela et al. (2021) investigates the so-called fall effect which spans a time range from summer solstice until the end of October and thus includes the October effect. They argue that the fall effect cannot be caused by space weather as those phenomena have either shorter (e.g., gamma-ray bursts, solar rotation) or longer time scales (e.g., solar cycle) or are non-recurring. Thus, changes in the neutral atmosphere dynamics seem to cause the October effect (Macotela et al., 2021).

The October effect and the fall effect have in common that they show a spring-fall asymmetry (Macotela et al., 2021), meaning that similar behavior cannot be observed during the spring transition. However, we would
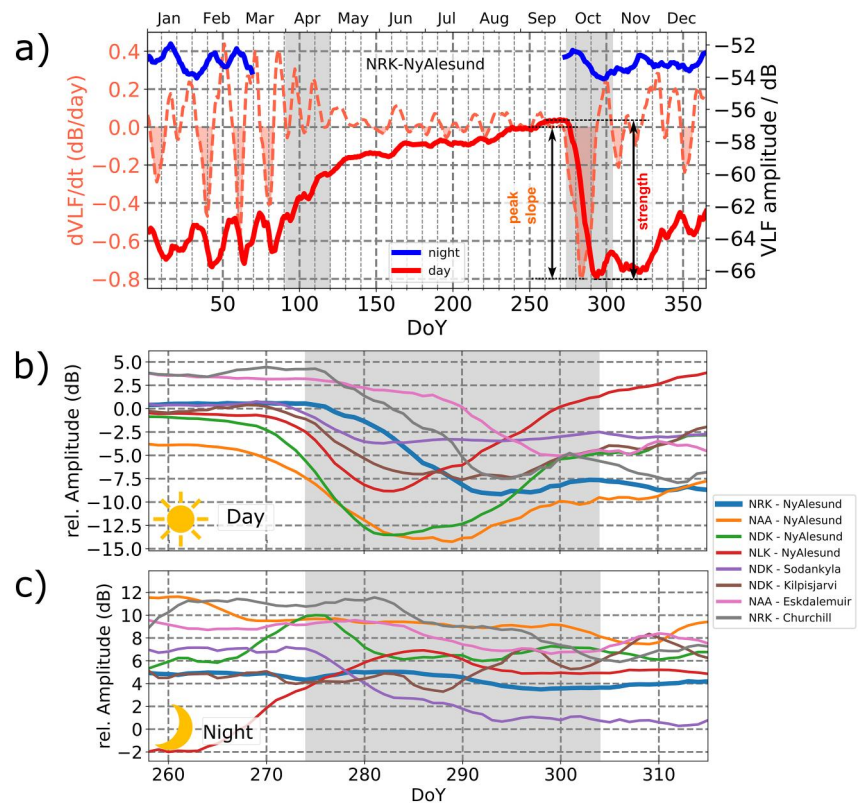
Figure 1. Average seasonal variation of (a) the VLF amplitude during daytime (red) and nighttime (blue) and the temporal gradient (first derivative) of the VLF daytime amplitude (dashed orange) for NRK-NyAlesund, (b) the daytime relative amplitude for different Tx-Rx combinations, (c) the nighttime relative amplitude for different Tx-Rx combinations. The months of April and October are highlighted in gray.

expect similar behavior in spring if the seasonal change of the solar zenith angle is the cause the October effect (Nicolet & Aikin, 1960).

Another striking feature of the October effect is that it only occurs during daytime (see Figure 1). This means that the strong and rapid decrease in the VLF amplitude can only be observed when the sun illuminates the D-region. No such rapid decrease in the VLF amplitude can be observed during nighttime. Therefore, the obvious question occurs, why does the October effect occur only during daytime and not during nighttime? Answering this question might help to bring us closer to explaining how and why the October effect occurs.

To find out why the October effect occurs only during daytime, we follow Macotela et al. (2021) and compare the occurrence of the VLF amplitude decrease with the characteristics of the neutral temperature in the mesosphere. The temperature is used for now as it seems to be a good proxy for the actual but unknown mechanism where atmospheric dynamics seem to play a key role (Macotela et al., 2021).

The paper is structured as follows: First, the here used observations and methods are described in Section 2. From different VLF observations, we obtain the average characteristics of the October effect in Section 3. In Section 4 the characteristics of temperature changes regarding the October effect are studied resulting in an answer to the key question of this paper. The results are then discussed in Section 5 and summarized in Section 6.

2. Data and Methods

To investigate the October effect systematically VLF signal amplitudes from different Transmitter-Receiver (Tx-Rx) combinations from the Antarctic Arctic Radiation-belt Dynamic Deposition VLF Atmospheric Research Konsortia (AARDDVARK) are investigated. AARDDVARK provides a network of continuous long-range observations of the lower ionosphere (Clilverd et al., 2009). Here, we combine four transmitters located in North America and Iceland (NAA, NDK, NLK, NRK) with six receivers, located in North America and Europe

(Churchill, Eskdalemuir, Kilpisjarvi, NyAlesund, Seattle, Sodankylä). A map with all Tx-Rx combinations including their midpoints is provided in Figure 4. For the single combinations, there are between 11 and 18 years of data available. Detailed information about the characteristics of the transmitter, location of the transmitter and receiver as well as the midpoints, path lengths, and data availability of the Tx-Rx combinations can be found in Supporting Information S1 (Tables S1–S5). Note that we use 10-min medians of the VLF signal amplitude raw data to reduce short-term fluctuations.

Considering long VLF signal time series can be problematic as they often contain jumps and outliers mainly caused by maintenance. Since we want to average over all available years per Tx-Rx combination to get the average characteristics of the October effect, the time series has to be continuous and without outliers. Therefore, we first apply the Pruned Extract Linear Timed (PELT) method (Killick et al., 2012) to detect and balance jumps automatically. Next, we apply a two-step outlier detection. In the first step, a band-pass filter is applied which filters out most of the regularly occurring maintenance outlier. In the second step, the median of all absolute deviations from the median (MAD; Rousseeuw & Hubert, 2011) method is applied in two dimensions. In the first dimension, the MAD method is applied to a running window of 60 days going through the whole time series. Using a shorter window size than 60 days would detect the VLF amplitude decrease during sunrise and sunset as an outlier while a longer window size would detect the October effect as an outlier. In the second dimension, the MAD method is applied to each time step comparing the different years. A value is detected as an outlier if it is detected as an outlier in both dimensions. A more detailed description of both methods can be found in and was first applied to VLF signals by Schneider et al. (2024).

The average seasonal variation of the VLF signal amplitude is obtained by applying the composite analysis to the average daytime (11–13 LT) and nighttime (22–24 LT) curves. Note, that additionally, nighttime means that no sunlight hits the D-region leading to data gaps in summer in polar latitudes due to polar day. To smooth the resulting curves the Savitzky-Golay filter (Luo et al., 2005) is applied with a polynomial order 3 and a window size of 15 days. Shorter window sizes lead to too noisy curves while longer window sizes smooth out the October effect. The above-described methods are applied to 22 Tx-Rx combinations. In the following section, the link NRK-NyAlesund is used exemplary to show the characteristics of the October effect in detail.

As we hypothesize that the October effect in VLF signal amplitudes is caused by neutral atmosphere dynamics, we compare the VLF signal amplitudes with global neutral temperature data from the Microwave Limb Sounder (MLS) on board the Aura satellite (Livesey et al., 2015; Waters et al., 2006). MLS has a global coverage from 82° S to 82°N on each orbit, and a useable height range from approximately 11 to 97 km (261–0.001 hPa) with a vertical resolution of ~4 km in the stratosphere and ~14 km at the mesopause height. The temporal resolution is 1 day at each location, and data are available from August 2004 until today (Livesey et al., 2015). Version 5 MLS data were used and the most recent recommended quality screening procedures of Livesey et al. (2015) have been applied. For our analyses, the original orbital MLS data are accumulated in grid boxes with 10° grid spacing in longitude and 5° in latitude. Afterward, they are averaged at every grid box and for every day, generally resulting in a global grid with values at every grid point.

3. Average Characteristics of October Effect

In order to find out why the October effect occurs during daytime only, we have to characterize this annual phenomenon. Since the variability among the available VLF Tx-Rx combinations is high, we will use several combinations located in the Northern Hemisphere focusing on polar latitudes. Figure 1a shows the average seasonal variation of the daytime (red) and nighttime (blue) VLF amplitude for the combination NRK-NyAlesund exemplary. The nighttime curve shows little seasonal variability and has a big gap in summer due to the polar day. The daytime curve shows a strong seasonal variability with distinctively higher values in summer than in winter. The increase in VLF amplitude in spring is significantly slower than the decrease in autumn, named the October effect, resulting in a spring-fall asymmetry. This spring-fall asymmetry is even more clearly visible in the temporal gradient (first derivative) of the daytime VLF amplitude (dashed orange line) where the October effect is characterized as the strongest negative peak in a year. The October effect is observed in various Tx-Rx combinations in the northern polar hemisphere. Note, that there is no gap in the daytime curve in winter during polar night as the D-region is still contaminated by solar radiation. During the winter solstice, the lowest solar zenith angle is about 95° at the surface at the midpoint between NRK and NyAlesund, that is, the sun does not rise. However, at 70 km the horizon is about 8° lower than at the surface meaning that the D-region is still sunlight
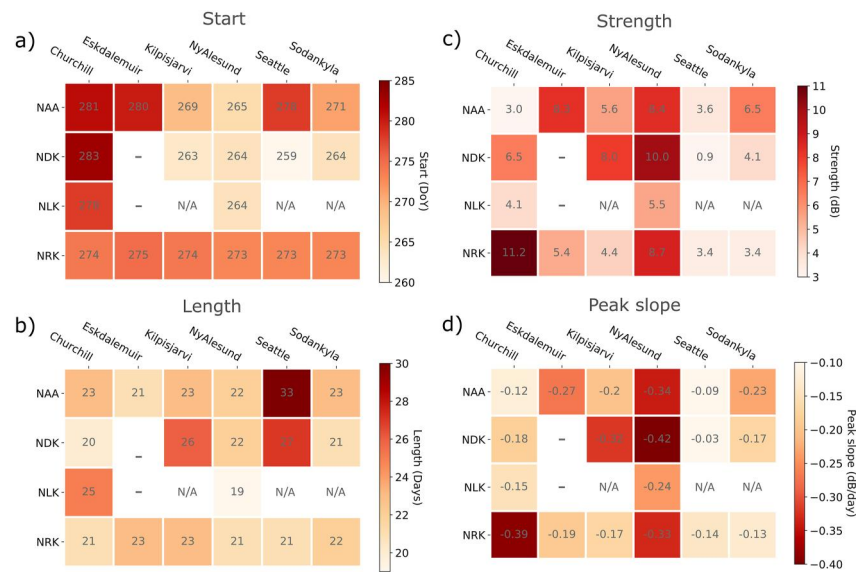
Figure 2. Heatmaps of the average (a) start of October effect, (b) length, (c) magnitude, and (d) peak slope of October effect for different Tx-Rx combinations. Note that "–" means that no data are available while "N/A" means that no October effect was detected.

around local noon at winter solstice. Thus, there is no gap in the VLF observations during the daytime in polar winter. Figure 1b shows average daytime VLF amplitudes for different Tx-Rx links during the fall transition. Note, that relative amplitudes are shown, that is, relative to the year mean, as the absolute amplitudes vary greatly between the combinations and thus make a comparison difficult. Additionally, for better visibility of the October effect, the curves are shifted such that all relative amplitudes are zero on the 15th of September. The daytime curves in Figure 1b show a strong decrease in October whereby the magnitude and the beginning of the decrease differ between the different Tx-Rx combinations. On average (mean over all links) there is a decrease of 7 dB (black dashed line) during daytime in the first half of October. The nighttime curves in Figure 1c vary with time but do not show such a uniform decrease as observed during the daytime. Thus, the October effect can be observed only during daytime and not nighttime (cf. black dashed lines in Figures 1b and 1c).

To get average characteristics of the start, end, and magnitude of the October effect we developed a simple method to detect the October effect automatically. In this method, we smooth the average amplitude curves with a Gaussian filter of width 7 and calculate the first and second derivatives (see Figures S1–S4 in Supporting Information S1 for all links). In the period between September 15 and November 5 (DoY 258–310), we first look for times when the first derivative is negative. If more than one time interval is detected the one with the lowest minimum which is longer than 5 days is taken to account for short-term solar or geomagnetic disturbances. Within this time interval, the minimum in the second derivative is then defined as the October effect beginning and the subsequent maximum as the end of the October effect. We applied this method to several Tx-Rx combinations in the northern polar hemisphere. Figure 2 gives an overview of the key characteristics of the October effect for combinations between the transmitter NAA, NDK, NLK, and NRK and the receiver Churchill, Eskdalemuir, Kilpisjarvi, NyAlesund, Seattle, and Sodankylä respectively. For these combinations, the October effect starts on average between DoY 259 and 283 and lasts between 20 and 33 days (see Figures 2a and 2b). For the period of the October effect, we define the magnitude of the October effect by the difference between the maximum and minimum of the VLF amplitude and the peak slope as the minimum in the first derivative (cf. Figure 1a). The average October effect magnitude ranges between 0.9 and 11.2 dB for the different combinations while the peak slope ranges between −0.03 and −0.42 dB/day (see Figures 2c and 2d).

In summary, the October effect occurs only during daytime and, when averaging over all combinations, the October effect starts on DoY 273 (±6 days), lasts for 22 (±3) days, and has a typical magnitude of 5.5 (±2.6) dB as well as an average peak slope of 0.19 (±0.1) dB/day.
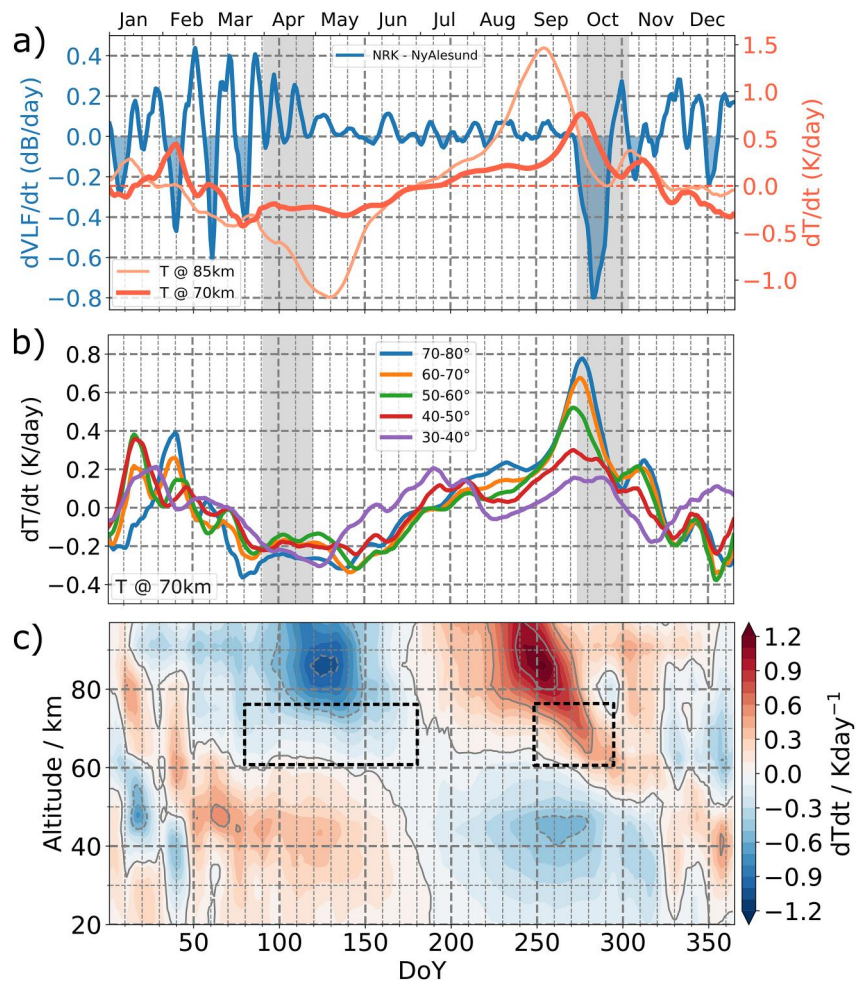
Figure 3. Composite of the temporal variation of the temporal gradient of (a) the VLF amplitude during daytime (blue) as well as the zonal mean temperature at 70 km (orange) and 80 km (light orange) both averaged between 60° and 70°N; (b) the zonal mean temperature at 70 km for different latitude bands. (c) Composite of the seasonal variation of the temporal gradient of the zonal mean temperature averaged between 60° and 70°N as a function of altitude. The temperature data are derived from MLS.

4. Atmospheric Impact on the October Effect

The mechanism of the October effect is currently unknown but there are strong hints that neutral atmosphere dynamics play a key role (Macotela et al., 2021). Following Macotela et al. (2021) we investigate the mesospheric temperature in the context of the VLF signal, again exemplary using the Tx-Rx combination NRK-NyAlesund. Figure 3a shows first the first derivative according to time of the VLF amplitude for NRK-NyAlesund (blue) whereby negative regions are highlighted by blue shading and second, the average temporal gradient of the zonal mean temperature averaged between 63° and 80°N, the latitude range of the VLF path, at 70 km (orange) and 85 km (light orange). Note, that these two altitudes represent the approximate daytime and nighttime VLF reflection heights respectively. At 85 km the seasonal temperature variation is roughly symmetric between spring and autumn with a cooling in spring of up to about −1.2 K/day and a warming in autumn also of up to about 1.46 K/day. At 70 km there is also a cooling in spring and a warming in autumn but their magnitude differs strongly. While in spring the cooling is up to −0.42 K/day, the warming in autumn is up to 0.76 K/day and thus almost twice as strong as in spring. Thus, similar to the daytime VLF signal, there is a spring-fall asymmetry in the seasonal variation of the temporal temperature gradient at 70 km. Note, that the temporal gradient of the VLF amplitude peaks about 1 week later as the warming at 70 km (caution: grid resolution in Figure 3 is 10 days) which gives a hint that other processes like atmospheric circulation changes and chemistry may also play a role.
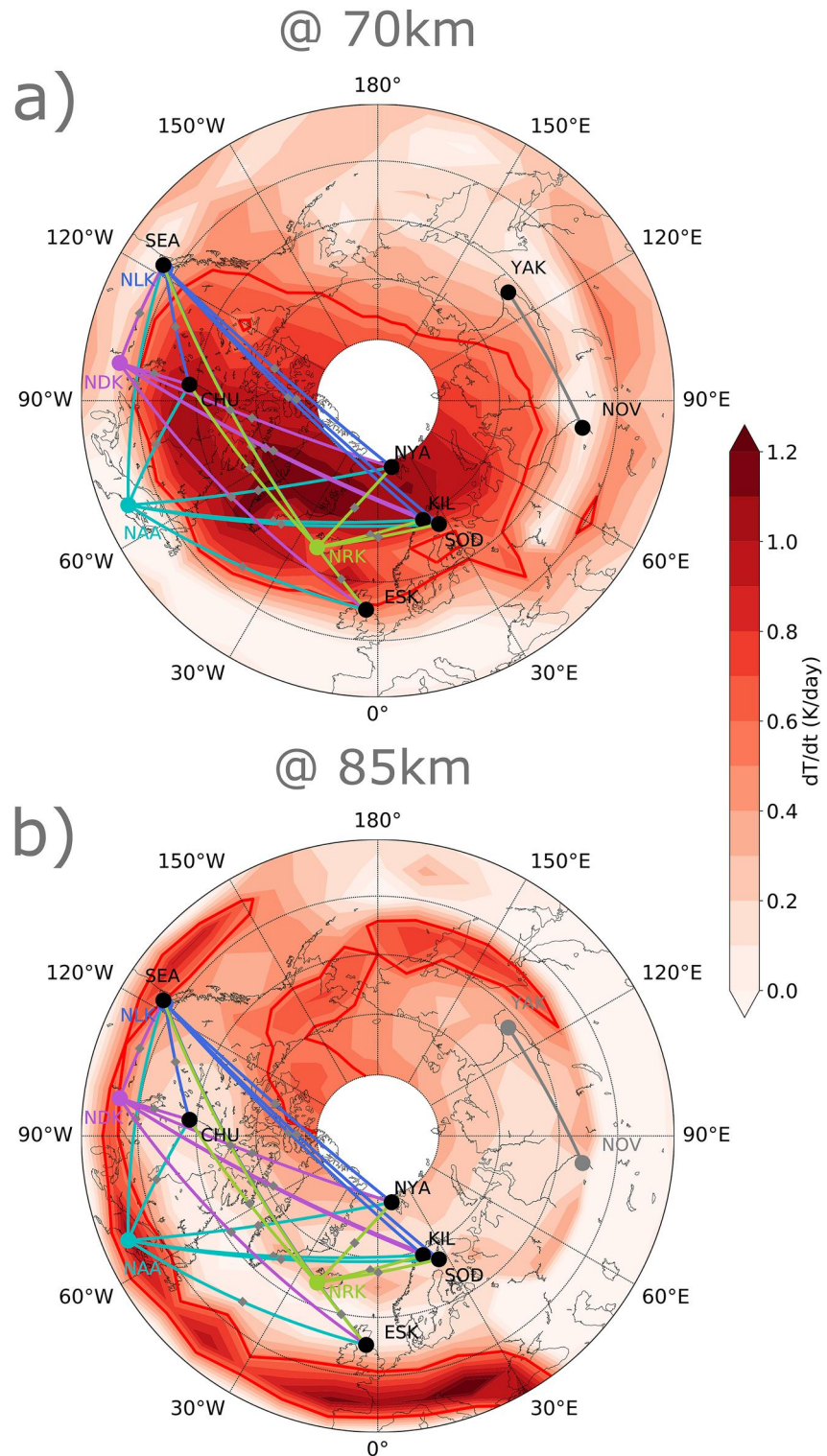
Figure 4. Composite of the temporal temperature gradient at (a) 70 km and (b) 85 km averaged around the peak of the October effect (doy 273–283). Links startings from different transmitter are marked in different colors (NAA—turquoise, NDK—purple, NLK—blue, NRK—green).

It is generally known, that the October effect in VLF observations can only be observed in mid and polar latitudes. Figure 3b shows the average temporal gradient of the zonal mean temperature at 70 km averaged over different latitude bands from low to polar latitudes. All latitude bands have in common that there is a cooling in spring and a

warming in fall. However, while the seasonal variation is symmetric between spring and fall equatorward of 50°N, it is asymmetric poleward of 50°N. Thus, the asymmetric temperature increase in fall occurs only poleward of 50°, and hence the temperature at 70 km behaves similarly to the October effect in VLF observations. This asymmetric temperature increase seems to be limited in altitude as it occurs at 70 km but not at 85 km (cf. Figure 3a). To find out in which altitude range the asymmetric warming occurs, Figure 3c shows the average temporal gradient of the zonal mean temperature averaged between 60° and 70°N as a function of day of year (DoY) and altitude. In the stratosphere (20–60 km) and upper mesosphere (75–100 km), there is symmetric behavior between spring and fall with a warming in spring and a cooling in fall and vice versa respectively. However, in the lower mesosphere, between approximately 60 and 75 km (dashed boxes), there is an asymmetry between spring and fall with a low cooling in spring and a strong warming in fall. The "tail," which can be observed in the fall, is not observable in a similar form in the spring, either before or after cooling (dashed rectangles in Figure 3c). In summary, there is an asymmetric warming in the lower mesosphere between 60 and 75 km in fall occurring poleward of 50° only. This warming has similar characteristics to the October effect suggesting that this regional asymmetric temperature increase plays a major role in the mechanism for the formation of the October effect.

Thus, the limited altitude range of the asymmetric warming in fall which does not follow the seasonal cycle of the solar zenith angle, is the reason for the occurrence of the October effect only during daytime and not during nighttime.

5. Discussion

It was shown, that the October effect occurs only during the daytime due to the limited altitude range of the asymmetric neutral temperature warming in fall. This warming is, as shown above, limited to the lower mesosphere and polar latitudes. However, the longitudinal expansion of the October effect is still unclear. Therefore, Figure 4a shows a map of the increased temporal temperature gradient at 70 km during the peak of the October effect, that is, the area where the asymmetric warming results in the October effect. Note, that the red thick line marks the level 0.55 dB/day to highlight the area of strong temperature increase. The area of increased temperature gradient extends from Europe over the Atlantic to North America. The Asian and Pacific regions are not influenced by this asymmetric temperature increase. Thus, we assume that Tx-Rx combinations whose great circle paths lie mostly in the Pacific and Asian regions would not show an October effect in their daytime VLF signal amplitude. Here, we cannot confirm this hypothesis as the AARDDVARK network has no Tx-Rx combinations covering this region. However, Korsakov et al. (2020) showed that there is no October effect in the seasonal variation of the daytime VLF signal amplitude between the transmitter in Novosibirsk and the receiver in Yakutsk. The great circle path between Novosibirsk (NOV) and Yakutsk (YAK) lies outside of the area with increased temperature (cf. Figure 4), so we would also not expect that an October effect can be observed there. This supports our hypothesis that the October effect can only be observed in areas with increased temperature during fall. Note, that at 85 km, the nighttime VLF reflection height, there is no such increase in the temporal temperature gradient during the October effect (see Figure 4b) as compared to 70 km. Thus, the dynamics responsible for the October effect act at 70 km only, that is, during the daytime.

Combinations between the transmitter NLK and the receivers Seattle, Kilpisjarvi, and Sodankylä do not show the October effect (cf. Figure 2) although their great circle paths lie within the area of increased temperature (cf. Figure 4). The receiver in Seattle is located very close to the transmitter NLK and thus we assume that the ground wave dominates the VLF observations (Thomson, 2010; Yoshida et al., 2008). For the other two receivers in northern Europe, the received VLF amplitude is weak and the seasonal variation has a wavy structure (not shown) which makes it difficult for the algorithm to detect the October effect. Additionally, we assume that the location of Kilpisjarvi, and Sodankylä toward NLK is unfavorable in the wave field leading to destructive modal interference and therefore to low amplitudes. However, the cause of the seasonal variation of the individual Tx-Rx combinations is beyond the scope of this study.

The warming that occurs at the VLF nighttime reflection height (∼85 km) during fall (cf. Figure 3c), is mainly driven by the seasonal solar zenith angle as it is symmetric between spring and fall. On the contrary, the regional asymmetric warming at VLF daytime reflection height (∼70 km) is not driven by the seasonal solar zenith angle. It is not clear if the temperature increase alone can be responsible for the observed strong decrease in the VLF amplitude. There are two known mechanisms for how the temperature can impact the VLF amplitude. The first one is destructive modal interference where the warming of the D-region leads to a downward displacement of the

VLF reflection height resulting in a change in the modal interference pattern and thus to a lower VLF amplitude (Silber et al., 2013). The second one is the VLF wave abortion where the warming leads to a higher collision frequency ν resulting in a stronger attenuation and thus a lower VLF amplitude (Macotela et al., 2021). While the first mechanism reduces the VLF amplitude by about 0.5 dB/km this is not known for the second mechanism (Silber et al., 2013). Thus, it is very likely that the temperature increase alone is not responsible for the strong decrease in the VLF amplitude. Further, we suspect that during the fall transition changes in the atmospheric meridional circulation drive changes in neutral temperature, and have an impact on the atmospheric chemistry (e.g., Dunkerton, 1978; Hoffmann et al., 2010; Matthias et al., 2015) resulting in changes in the electron density and therefore in the amplitude of subionospheric propagating VLF waves (Clilverd et al., 2001).

6. Summary and Conclusion

In summary, there is a rapid decrease in the daytime VLF signal amplitudes during October in polar latitudes which is long known as the October effect. In this study we showed that the average October effect starts on day 273, lasts for 22 days, and has a magnitude of 5.5 dB as well as a peak slope of 0.19 dB/day. While the mechanism behind the October effect is currently unknown, geomagnetic and solar causes can be ruled out as their time scales are either too long or too short (Macotela et al., 2021). Therefore, neutral atmosphere dynamics seem to play a major role. Warming, which is limited to the lower mesosphere and asymmetric between spring and fall, seems to play a major role in the mechanism resulting in the October effect in VLF signals. This warming occurs also in polar latitudes only and is limited to the altitude range between 60 and 75 km, the daytime VLF reflection height. Finally, we can answer why does the October effect not occur at night. The October effect cannot be observed during nighttime since the warming, playing a key role in its formation mechanism, is limited to the lower mesosphere and thus is located below the nighttime VLF reflection height.

Data Availability Statement

All data used in this study are freely available. VLF signal data are available from AARDDVARK Network (2009). Aura MLS data is available from Schwartz et al. (2020).

References

AARDDVARK Network. (2009). VLF radio waves observations in Arctic and Antarctic region [Dataset]. Retrieved from https://psddb.nerc-bas.ac.uk

Banks, L., & Kockarts (1973). *Aeronomy*. Academic Press. Nan (Ed.).

Barr, R. (1971). The propagation of ELF and VLF radio waves beneath an inhomogeneous anisotropic ionosphere. *Journal of Atmospheric and Terrestrial Physics*, *33*(3), 343–353. https://doi.org/10.1016/0021-9169(71)90139-5

Chapman, F. W., & Macario, R. C. V. (1956). Propagation of audio-frequency radio waves to great distances. *Nature*, *177*(4516), 930–933. https://doi.org/10.1038/177930a0

Clilverd, M. A., Rodger, C. J., Gamble, R. J., Ulich, T., Raita, T., Seppälä, A., et al. (2010). Ground-based estimates of outer radiation belt energetic electron precipitation fluxes into the atmosphere. *Journal of Geophysical Research*, *115*(A12), A12304. https://doi.org/10.1029/2010JA015638

Clilverd, M. A., Rodger, C. J., Thomson, N. R., Brundell, J. B., Ulich, T., Lichtenberger, J., et al. (2009). Remote sensing space weather events: Antarctic-Arctic radiation-belt (dynamic) deposition-VLF atmospheric research konsortium network. *Space Weather*, *7*(4). https://doi.org/10.1029/2008sw000412

Clilverd, M. A., Rodger, C. J., Thomson, N. R., Lichtenberger, J., Steinbach, P., Cannon, P., & Angling, M. J. (2001). Total solar eclipse effects on VLF signals: Observations and modeling. *Radio Science*, *36*(4), 773–788. https://doi.org/10.1029/2000RS002395

Dunkerton, T. (1978). On the mean meridional mass motions of the stratosphere and mesosphere. *Journal of the Atmospheric Sciences*, *35*(12), 2325–2333. https://doi.org/10.1175/1520-0469(1978)035⟨2325:OTMMMM⟩2.0.CO;2

Hoffmann, P., Becker, E., Singer, W., & Placke, M. (2010). Seasonal variation of mesospheric waves at northern middle and high latitudes. *Journal of Atmospheric and Solar-Terrestrial Physics*, *72*(14), 1068–1079. https://doi.org/10.1016/j.jastp.2010.07.002

Killick, R., Fearnhead, P., & Eckley, I. A. (2012). Optimal detection of changepoints with a linear computational cost. *Journal of the American Statistical Association*, *107*(500), 1590–1598. https://doi.org/10.1080/01621459.2012.737745

Korsakov, A. A., Kozlov, V. I., & Toropov, A. A. (2020). Seasonal variations of the amplitude of the VLF radio signals and the intensity of the atmospheric electric field in Cryolithozone conditions. *IOP Conference Series: Materials Science and Engineering*, *753*(4), 042093. https://doi.org/10.1088/1757-899X/753/4/042093

Livesey, N. J., Read, W. G., Wagner, P. A., Froidevaux, L., Lambert, A., Manney, G. L., et al. (2015). *EOS MLS version 4.2x level 2 data quality and description document*. Jet Propulsion Laboratory, California Institute of Technology, Pasadena, CA.

Luo, J., Ying, K., & Bai, J. (2005). Savitzky–golay smoothing and differentiation filter for even number data. *Signal Processing*, *85*(7), 1429–1434. https://doi.org/10.1016/j.sigpro.2005.02.002

Macotela, E. L., Clilverd, M., Renkwitz, T., Chau, J., Manninen, J., & Banyś, D. (2021). Spring-fall asymmetry in VLF amplitudes recorded in the North Atlantic region: The fall-effect. *Geophysical Research Letters*, *48*(16), e2021GL094581. https://doi.org/10.1029/2021gl094581

Matthias, V., Shepherd, T. G., Hoffmann, P., & Rapp, M. (2015). The hiccup: A dynamical coupling process during the autumn transition in the Northern Hemisphere: Similarities and differences to sudden stratospheric warmings. *Annales Geophysicae*, *33*(2), 199–206. https://doi.org/10.5194/angeo-33-199-2015

Nicolet, M., & Aikin, A. C. (1960). The formation of the D region of the ionosphere. *Journal of Geophysical Research*, *65*(5), 1469–1483. https://doi.org/10.1029/JZ065i005p01469

Pancheva, D. V., & Mukhtarov, P. Y. (1996). Modelling of the electron density height profiles in the mid-latitude ionospheric D-region. *Annales Geophysicae*, *39*(4). https://doi.org/10.4401/ag-4021

Rousseeuw, P. J., & Hubert, M. (2011). Robust statistics for outlier detection. *WIREs Data Mining and Knowledge Discovery*, *1*(1), 73–79. https://doi.org/10.1002/widm.2

Schneider, H., Wendt, V., Banys, D., Clilverd, M., & Raita, T. (2024). Processing of VLF amplitude measurements: Deduction of a quiet time seasonal variation. *Radio Science*, *59*(2). https://doi.org/10.1029/2023RS007834

Schwartz, L. N., Livesey, N., & Read, W. (2020). *MLS/aura level 2 temperature v005*. Goddard Earth Sciences Data and Information Services Center (GES DISC). https://doi.org/10.5067/Aura/MLS/DATA2520

Silber, I., Price, C., Rodger, C. J., & Haldoupis, C. (2013). Links between mesopause temperatures and ground-based VLF narrowband radio signals. *Journal of Geophysical Research: Atmospheres*, *118*(10), 4244–4255. https://doi.org/10.1002/jgrd.50379

Thomson, N. R. (2010). Daytime tropical D region parameters from short path VLF phase and amplitude. *Journal of Geophysical Research*, *115*(A9), A09313. https://doi.org/10.1029/2010JA015355

Thomson, N. R., & Clilverd, M. A. (2000). Solar cycle changes in daytime VLF subionospheric attenuation. *Journal of Atmospheric and Solar-Terrestrial Physics*, *62*(7), 601–608. https://doi.org/10.1016/S1364-6826(00)00026-2

Wait, J. R., & Spies, K. P. (1964). Characteristics of the Earth-ionosphere waveguide for VLF radio waves. NBS Technical Note US, *300*, 100.

Waters, J. W., Froidevaux, L., Harwood, R. S., Jarnot, R. F., Pickett, H. M., Read, W. G., et al. (2006). The Earth observing system microwave limb sounder (EOS MLS) on the Aura satellite. *IEEE Transactions on Geoscience and Remote Sensing*, *44*(5), 1075–1092. https://doi.org/10.1109/TGRS.2006.873771

Yoshida, M., Yamauchi, T., Horie, T., & Hayakawa, M. (2008). On the generation mechanism of terminator times in subionospheric VLF/LF propagation and its possible application to seismogenic effects. *Natural Hazards and Earth System Sciences*, *8*(1), 129–134. https://doi.org/10.5194/nhess-8-129-2008